Journal of Applied Mechanics and Technical Physics, Vol. 37, No. 6, 1996

EVAPORATION DYNAMICS AT SUPERATMOSPHERIC PRESSURE

B. P. Avksentyuk and V. V. Ovchinnikov

UDC 536.248

1. Introduction. Despite numerous studies of the physics of boiling, the calculation of the dynamics of transient processes (vapor explosion, explosive boiling, heat-transfer crisis, transition boiling, and flashing) still remains problematic. This is due not only to the difficulties in describing them by a system of hydrodynamics and heat-transfer equations and in solving this system, but also to an incomplete understanding of the physical factors affecting these processes. The latter is largely accounted for by the absence of fundamental experimental studies that could form the basis for creating adequate theoretical models. Transient processes in boiling systems usually occur at high levels of metastability of a liquid. To understand these complex processes, it is necessary to study the dynamics of evaporation at high superheatings of a liquid.

In [1], it was first shown that under strong superheatings of the heating surface relative to the saturation temperature, the disintegration of a metastable near-wall liquid proceeds in the form of evaporation fronts spreading along a heater with high constant velocity. Evaporation fronts appear on the surface of a vapor bubble as a result of the loss of interphase-surface stability [2]. The term "evaporation front" is used for the face part of the surface of a vapor formation spreading along the heater. In [3–6], the effect of the regime parameters (superheating, pressure, and subcooling) on the velocity of an evaporation front in water and organic liquids at subatmospheric pressures was studied experimentally. At low pressures a critical regime of vapor outflow from an evaporation front occurs. To describe the evaporation front under these conditions, a model was created based on a simplified theory of evaporation using the Hertz–Knudsen formula for vapor mass flow.

The authors of the present paper and [7] performed experiments on evaporation dynamics at atmospheric pressure only under strong subcoolings of a bulk liquid to the saturation temperature. Subcooling has an essential effect on the size of a vapor formation. It is therefore difficult to trace, under these conditions, the effect exerted by a change in the regime of vapor outflow on the evaporation-front velocity. The data on the evaporation-front velocity at superatmospheric pressures are given in [8, 9] where the heat-transfer crises in R113 during stepwise power generation were studied. Unfortunately, the authors do not mention under what superheatings the data were obtained.

Below, we present the results of studies of the dynamics of interphase surfaces during explosive boiling at superatmospheric pressure when there occurred a subcritical regime of vapor outflow from an evaporation front. We also give a physical model of an evaporation front based on the nonequilibrium theory of evaporation. This theory makes it possible to calculate actual vapor parameters near the evaporation surface.

2. Experimental Setup and Measurement Technique. The experimental setup used to investigate the process of boiling is schematically depicted in Fig. 1. A test heater 1 was a stainless steel tube with external diameter 2.5 mm, length 82 mm, and wall thickness 0.5 mm. Inside the tube there was a thermocouple, whose thermoelectromotive force was measured with a digital voltmeter 7. In determining the heating-surface temperature, a correction was introduced to take into account the temperature drop in the wall. The test heater in the liquid volume was installed horizontally and was heated quasi-steadily by supplying an alternating current of 50 Hz directly from a source 6. A working volume 2 contained about 5 liters of working liquid (freon C318). In the working volume there were windows made of heat-resistant glass for visual observation and camera recording. A piezoelectric pressure gauge 3 was attached to the current supply of the test heater.

Kutateladze Institute of Thermal Physics, Siberian Division, Russian Academy of Sciences, Novosibirsk 630090. Translated from Prikladnaya Mekhanika i Tekhnicheskaya Fizika, Vol. 37, No. 6, pp. 91–98, November–December, 1996. Original article submitted May 29, 1995; revision submitted August 28, 1995.

 0021-8944/96/3706-0850 $15.00

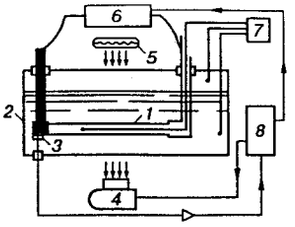

Fig. 1

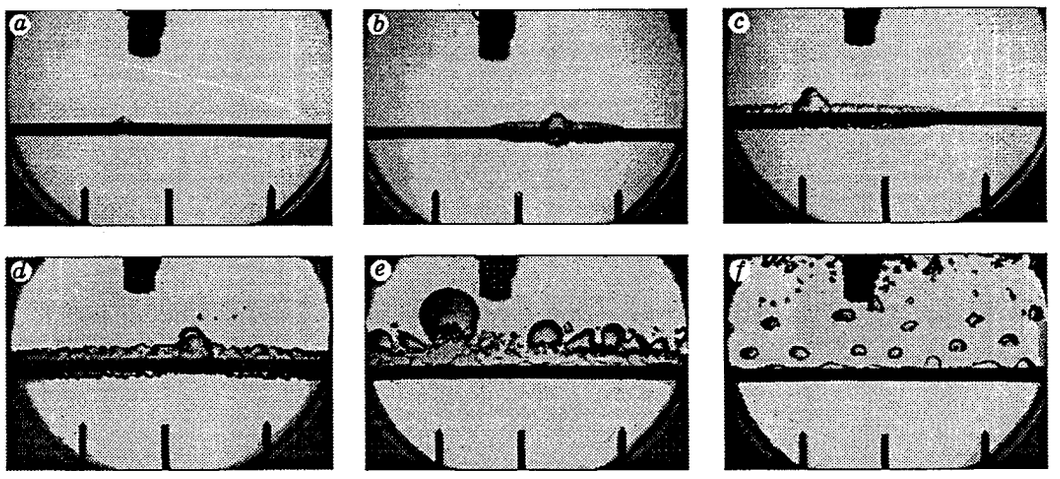

Fig. 2

A signal produced in it when freon C318 boiled came through an amplifier to a triangular-pulse-formation scheme 8. This pulse was used to open the shutter of the camera, to trigger a flash bulb 5 during camera recording, and to switch off the electric heating of the test heater after a preset delay time.

Camera recordings were performed with a high-speed camera 4 at a rate of 5500 frames/sec, and one recording lasted 13 msec. The test heater was de-energized 30 msec after the onset of boiling. In processing the films, in each camera record measurements were made of the transverse dimension h of the initial bubble and the longitudinal dimension L of the vapor formation from the point at which the first bubble appeared to the evaporation front. The experiments were made at the saturation temperature under conditions of natural convection. During the experiments the heat-flux density, the temperature of the test-heater surface before boiling, the temperature of the liquid and of the vapor, and the pressure in the working volume were measured.

3. Experimental Results. The experiments were performed at pressures of $2.5 \cdot 10^5$–$2.8 \cdot 10^5$ Pa in the working volume. Superheatings before boiling did not exceed 56 K, but even under such weak superheatings the changes of the vaporization structure in freon C318 were observed. The threshold value of superheating amounted to 40 K. For superheating values below the threshold, upon boiling ordinary vapor bubbles grew on the heater surface and detached from it. Under stronger superheating the evaporation fronts arose on the surface of a bubble near the heater and spread along the heater surface.

Figure 2 shows the camera records of freon C318 boiling under superheatings above the threshold value. One camera recording was made for each boiling. The light background refers to the liquid, the horizontal dark streak to the test heater, and under the latter there are scale marks. Table 1 lists the regime parameters at which the records were taken: T_s is the saturation temperature corresponding to the pressure in the working volume before boiling P_∞, $\Delta T = T_w - T_s$ is the superheating before boiling (T_w is the temperature of the test-heater surface before boiling), and τ is the delay time. The moment at which a signal appeared in the pressure gauge fixed to the current supply of the test heater was considered the reference time.

Figure 2a shows the stage of formation of evaporation fronts on the surface of a bubble at its base. Propagation of the evaporation fronts can be seen in Figs. 2b and 2c. After the evaporation fronts had

TABLE 1

Notations in Fig. 2	ΔT, K	T_s, K	τ, msec	Notations in Fig. 2	ΔT, K	T_s, K	τ, msec
a	57.1	293.9	0.061	d	56.3	294.4	6.835
b	51.9	293.6	2.809	e	55.6	295.0	42.4
c	50.7	294.9	6.629	f	55.7	295.3	142.6

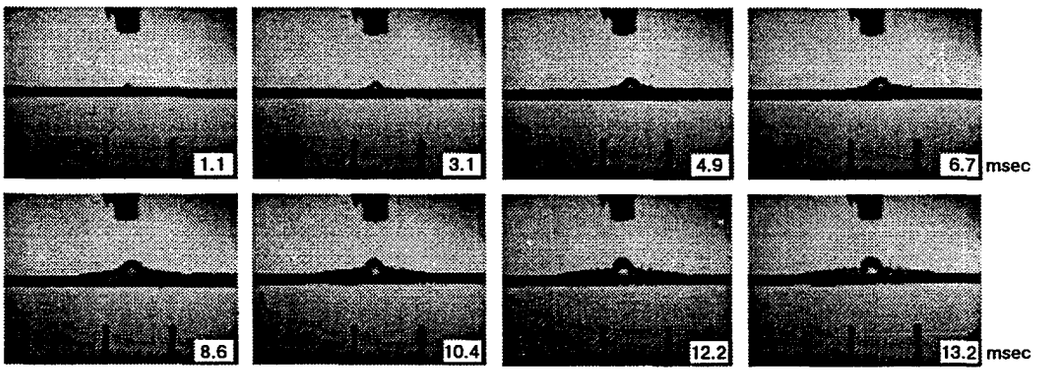

Fig. 3

spread over the entire heat-liberating surface, the transverse size of the vapor formation continued to increase (Fig. 2d). Before the vapor formation detached from the heater, it became unstable and broke into separate bubbles (Fig. 2e). The residual layer of the liquid on the heater separated from the bulk of the liquid by the vapor formation rapidly evaporated. Then, the temperature of the heater elevated. After the vapor formations had detached from the heater, a film boiling regime established on the heater (Fig. 2f).

High-speed recording of the boiling process made it possible to follow the changes in the size of a vapor formation in time. Figure 3 shows the characteristic records of the process of freon C318 boiling at a superheating of 41.9 K and a pressure of $2.5 \cdot 10^5$ Pa. For each record, the time from the onset of boiling is given. The results of processing of this recording are shown in Fig. 4, where the length L of the vapor formation, the diameter h of the bubble, and the rates of changes in these sizes are shown depending on the time τ: $v_f = \partial L/\partial\tau$ and $v_h = \partial(h/2)/\partial\tau$. The longitudinal size of the vapor formation increased as a linear function of time. This means that the evaporation-front velocity was constant. The transversal size varied in time by the law $\tau^{0.58}$.

In a number of cases, under superheating before boiling in excess of the threshold values the coexistence of two vaporization processes was observed: the spread of the evaporation and boiling fronts. By the boiling front, a chain process of boiling is meant when a growing bubble initiates, in its vicinity, the formation of another bubble on the heater.

Figure 5 shows the results of the processing of boiling records at a superheating of 48.6 K and a pressure of $2.6 \cdot 10^5$ Pa. In this case, 1 msec after the onset of boiling from one side of the initial bubble an evaporation front began to spread along the heater at a constant velocity of 3.1 m/sec, and from its other side a process of successive formation of the other bubbles began. In 4.5 msec, bubble formation stopped and another evaporation front began to propagate along the heater with the same velocity as the evaporation front spreading from the opposite side of the first bubble.

Thus, at superatmospheric pressures, just as at subatmospheric ones, the evaporation-front velocity is constant in time. Figure 6 shows the data on the evaporation-front velocity versus superheating before boiling for freon C318 at pressures of $2.5 \cdot 10^5$–$2.8 \cdot 10^5$ Pa. With an increase in superheating, the evaporation-front velocity also increases.

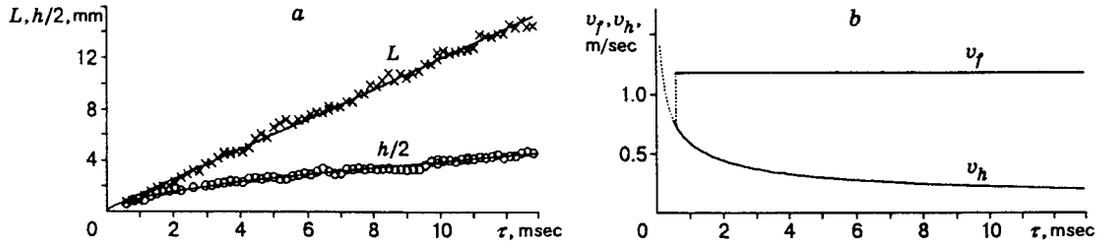

Fig. 4

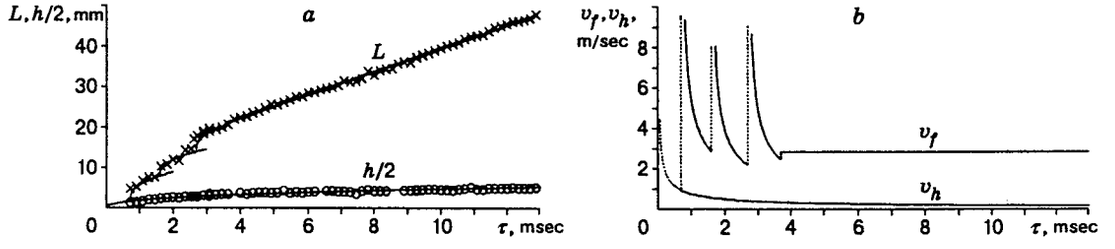

Fig. 5

4. The Evaporation-Front Model. A thorough description of the growth of a vapor formation of an unknown shape with a nonuniform temperature field in the near-wall layer where the effect of viscosity in a liquid is already profound is extremely complicated. To describe the propagation velocity of an evaporation front, it is sufficient, under certain assumptions, to consider only the face part (the vicinity of the critical point) of the vapor-formation surface.

In a metastable liquid, the evaporation front propagates with a constant velocity v_f which is one order of magnitude higher than that of liquid evaporation. Let us consider a test volume surrounding an evaporation front in a moving coordinate system fixed to the evaporation front (Fig. 7). In this coordinate system, the superheated liquid flows to the front from the left, while the vapor moves to the right from the evaporation surface.

We shall denote the velocity, pressure, and temperature of the liquid at infinity by v_f, P_∞, and T_w, respectively, and the pressure and the saturation temperature in the vapor region at infinity by P_∞ and T_s. At the critical point on the evaporation front, the liquid velocity is equal to that of its evaporation v_0. Here the pressure from the side of the liquid reaches the highest value P_0. We denote the liquid temperature on the evaporation front by T_0. The vapor velocity, pressure, temperature, and density in the vapor region on the outer side of the Knudsen layer are denoted by v_1, P_1, T_1, and ρ_{v1}, respectively, and the basic radii of the interface curvature on the evaporation front by $r_{1,2}$.

The evaporation surface of a liquid is a surface of discontinuity in passing through which the normal velocity component, pressure, density, and enthalpy undergo a discontinuity. For the frontal part of the interface (evaporation front), the conservation laws of the mass, momentum, and energy fluxes are the same as for shock waves:

$$j = \rho_{l0} v_0 = \rho_{v1} v_1; \tag{4.1}$$

$$P_0 + \rho_{l0} v_0^2 = P_1 + \rho_{v1} v_1^2 - \sigma_0 (1/r_1 + l/r_2); \tag{4.2}$$

$$j(i_1 - i_0) + j(v_1^2 - v_0^2)/2 - \lambda_{l0} \nabla T_0 + \lambda_{v1} \nabla T_1 = 0. \tag{4.3}$$

Here j is the mass flux of a substance; σ is the surface tension; i is the enthalpy; λ is the thermal conductivity; the subscripts l and v refer to the properties of the liquid and vapor; the subscript 0 refers to the values of the quantities on the discontinuity surface from the side of the liquid, and the subscript 1 refers to those on the interface from the side of the vapor. Equation (4.2) is written with allowance for the interface curvature.

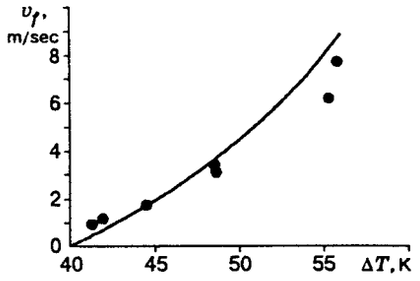

Fig. 6

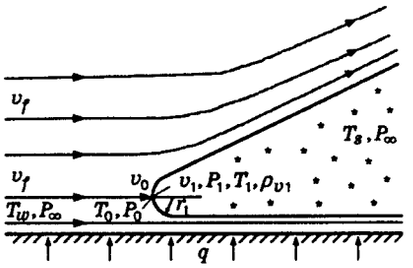

Fig. 7

In a nonviscous approximation, the equation of motion of a liquid reduces to the Bernoulli equation which for the central part of the flow, has the form

$$P_\infty + \rho_{l0} v_f^2/2 = P_0 + \rho_{l0} v_0^2/2. \tag{4.4}$$

From Eqs. (4.1), (4.2), and (4.4) for the evaporation-front velocity, we obtain

$$v_f = \sqrt{2\{j^2[1/\rho_{v1} - 1/(2\rho_{l0})] + P_1 - P_\infty - \sigma_0(1/r_1 + 1/r_2)\}/\rho_{l0}}.$$

An accurate determination of the basic radii of the evaporation-front curvature is a complicated task. The temperature distribution on the face part of the interface is not uniform. The surface temperature varies from the maximum value T_0 at the critical point to T_s. This gives rise to a nonuniform distribution of the forces with which the liquid and the vapor act on each other. Since the data on the temperature distribution over the interface in the neighborhood of the critical point are not yet available so far, in determining the radii of the evaporation-front curvature the following assumption was made: the pressure difference $(P_1 - P_\infty)$ is compensated for by surface tension, and the evaporation-front propagation is due to vapor recoil, i.e., inertial forces are compensated for by reactive ones. Then, writing the expression for the basic curvature radii in the form $r_{1,2} = 2\sigma_0/(P_1 - P_\infty)$, we find the final equation for the calculation of the evaporation-front velocity $v_f = j\sqrt{2[1/\rho_{v1} - 1/(2\rho_{l0})]/\rho_{l0}}$.

In the equation of energy-flux conservation (4.3), energy dissipation due to viscosity was ignored. An increase in the kinetic energy [the second term on the left-hand side of Eq. (4.3)] and heat removal from the discontinuity surface to the vapor region (the fourth term) can also be ignored, because taking them into account does not appreciably affect the calculation results. The difference between the enthalpies in Eq. (4.3) is equal to the latent heat of evaporation and should be found with allowance for the metastability of the liquid on the discontinuity surface $i_1 - i_0 = \tilde{H}$ and $\tilde{H} = H_{s1} - (c_{pl0}T_0 - c_{pls1}T_{s1})$. Here H_{s1} and c_{pls1} are the latent heat of evaporation and the specific heat at the saturation temperature T_{s1} corresponding to the vapor pressure P_1 on the outer side of the Knudsen layer.

The temperature gradient on the discontinuity surface from the side of the liquid phase is determined taking into account the evaporation in a heat-transfer approximation in the neighborhood of the front critical point when the liquid flows past a sphere with a radius equal to the main radius of the evaporation-front curvature. The equation of convective heat exchange in a boundary-layer approximation has the form

$$u\partial T/\partial x + v\partial T/\partial y = a_l \partial^2 T/\partial y^2, \quad y = 0, \quad T = T_0; \quad y \to \infty, \quad T = T_w. \tag{4.5}$$

In the vicinity of the critical point the surface is equally accessible [10]: the solution is independent of x and, hence, the first term in Eq. (4.5) can be ignored. Expressing the longitudinal and transverse components of the liquid velocity for this region in the form $u = Ux/r_1$, $v = -Uy/r_1 - v_0$, substituting their values into Eq. (4.5), and integrating it, we obtain an expression for the temperature gradient on the discontinuity surface

TABLE 2

T_s	ΔT	T_0	T_1	P_∞	P_1	v_f,	S	M	Re
K				kPa		m/sec			
293	40.2	293.04	292.7	264.1	265.2	0.07	1.02	0.01	3.5
293	44.0	298.40	291.7	264.1	286.3	1.49	1.13	0.07	3.5
293	48.0	304.90	290.6	264.1	312.8	3.34	1.29	0.15	3.4
293	52.0	312.40	289.4	264.1	345.3	5.69	1.48	0.25	3.2
293	56.0	324.40	288.0	264.1	386.8	8.87	1.74	0.36	3.0

from the side of the liquid:

$$\nabla T_0 = \sqrt{U/(2a_{l0}r_1)}(T_w - T_0)\exp(-b_1)\Big/\int\limits_{\sqrt{b_1}}^{\infty}\exp(-\eta^2)d\eta.$$

Here $b_1 = v_0^2 r_1/(2a_{l0}U)$ and a_{l0} is the thermal diffusivity of the liquid. For freon C318 in the studied range of parameters, the Reynolds numbers ($\mathrm{Re} = 2\nu_f r_1/v_{l0}$) are of order 3 (Table 2), which corresponds to a viscous-flow regime. Under these conditions, $U = v_f\mu_{l0}/[2(\mu_{l0} + \mu_{v0})]$ [10]. Thus, for the process considered, the equation of energy-flux conservation takes the form

$$j\tilde{H} = \sqrt{v_f\lambda_{l0}c_{l0}\rho_{l0}\mu_{l0}/[4r_1(\mu_{l0} + \mu_{v0})]}\,(T_w - T_0)\exp(-b)\Big/\int\limits_{\sqrt{b}}^{\infty}\exp(-\eta^2)d\eta \qquad (4.6)$$

$$[b = v_0^2 r_1(\mu_{l0} + \mu_{v0})/(v_f a_{l0}\mu_{l0})].$$

Equation (4.6) was used to determine the temperature of the liquid in the evaporation front.

The relationship between the vapor parameters on the evaporation-front surface and on the outer boundary of the Knudsen layer was approximated using the relations derived in [11]:

$$1 - T_1/T_0 = v_1\sqrt{\pi M/(2RT_0)}/4, \quad 1 - T_1/T_0 = 0.265\,(\rho_{v0s} - \rho_{v1})/\sqrt{\rho_{v0s}\rho_{v1}} \qquad (4.7)$$

(M is the molecular mass, R is the universal gas constant, and ρ_{v0s} is the vapor density on the saturation line at temperature T_0). Relations (4.7) are written assuming that $\beta = 1$ (β is the evaporation coefficient). In [12], it was shown that on a fresh evaporation surface the evaporation coefficient of various liquids is close to unity. This is due to a slow process of establishment of the equilibrium surface properties. The evaporation front is a fresh surface, since fronts occur only at high intensities of evaporation. To determine the vapor pressure on the outer side of the Knudsen layer, use was made of the equation of state given in [13]. The possibility of volumetric vapor condensation was not considered.

The vapor velocity on the outer side of the Knudsen layer is equal to the local sound velocity if the pressure P_1 exceeds considerably the ambient pressure P_∞. For high counterpressure, the vapor velocity is less than the sound velocity and is related to a pressure jump in the shock-wave front by the equation [14, 15] $F = (P_1 - P_\infty)\sqrt{2/\{\rho_{v\infty}[P_1(\gamma_\infty + 1) + P_\infty(\gamma_\infty - 1)]\}}$ (γ is the specific heat ratio of vapor). Thus, in calculations the desired relationship between v_1, ρ_{v1}, and T_1 was determined by the relations [16] $v_1 = u_1$ for $u_1 \leqslant F$ and $v_1 = F$ for $u_1 > F$, where $u_1 = \sqrt{\gamma_1 RT_1/M}$ is the local sound velocity.

Calculations according to the model described above were made at $T_s = 293$ K. The calculation results are listed in Table 2 and are shown by the curve in Fig. 6. All the experimental data (points) for freon C318 were obtained in a subcritical regime of vapor outflow from the evaporation front. The value of the Mach number M varied from 0.03 to 0.36. Table 2 presents the degrees of vapor oversaturation $S = P_1/P_{s1}$ (P_{s1} is the pressure of the saturated vapor at the temperature T_1) on the outer side of the Knudsen layer. Calculations by the model considered were also made using the nonequilibrium theory of evaporation [17]. In this case, the v_f values proved to be close to those presented in Fig. 6, but the vapor on the outer side of the Knudsen layer

turned out to be superheated.

In Fig. 6, the model is shown to describe correctly the influence of superheating on the propagation velocity of an evaporation front. The model also contains information on the threshold character of the appearance of evaporation fronts. The calculated threshold value of superheating at $T_s = 293$ K amounted to 40.2 K.

This work was supported by the Russian Foundation for Fundamental Research (Grant 95-02-04700).

REFERENCES

1. B. P. Avksentyuk, G. I. Bobrovich, S. S. Kutateladze, and V. N. Moskvicheva, "Degeneration of bubble boiling under conditions of free convection," *Prikl. Mekh. Tekh. Fiz.*, No. 1, 69–72 (1972).
2. J. E. Shepherd and B. Sturtevant, "Rapid evaporation at the superheat limit," *J. Fluid Mech.*, **121** 379–402 (1982).
3. B. P. Avksentyuk, V. V. Ovchinnikov, and V. Ya. Plotnikov, "Dynamics of boiling in the high-superheat region," in: *Heat Exchange in Vapor Generators*, Materials of All-Union Conference, Novosibirsk (1988), pp. 304–308.
4. B. P. Avksentyuk, V. V. Ovchinnikov, and V. Ya. Plotnikov, "Dynamics effects on interphase surface during the disintegration of superheated near-wall liquid," in: *Proc. Int. Cent. Heat Mass Transfer*, **33** (1991), pp. 583–598.
5. B. P. Avksentyuk and V. V. Ovchinnikov, "Evaporation dynamics in water," *Sib. Fiz.-Tekh. Zh.*, No. 1, 3–9 (1992).
6. B. P. Avksentyuk and V. V. Ovchinnikov, "A study of evaporation structure at high superheatings," *Russ. J. Eng. Thermophys.*, **3**, No. 1, 21–39 (1993).
7. S. A. Zhukov and V. V. Barelko, "On the autowave mechanism of decay of metastable heat-transfer regimes in the process of boiling," *Teplofiz. Vys. Temp.*, **27**, No. 5, 920–930 (1989).
8. J. Kozawa and S. Aoki, "Boiling transition phenomena and heat removal limits at transient high power generation," in: *Research of Effective Use of Thermal Energy*, Spey 14, Japan (1985), pp. 105–112.
9. K. Okuyama, Y. Kozawa, A. Inoue, and S. Aoki, "Transient boiling heat transfer characteristics of R113 at large stepwise power generation," *Int. J. Heat Mass Transfer*, **31**, No. 10, 2161–2174 (1988).
10. V. G. Levich, *Physicochemical Hydrodynamics* [in Russian], Fizmatgiz, Moscow (1959).
11. D. A. Labuntsov and A. P. Kryukov, "Analysis of intense evaporation and condensation," *Int. J. Heat Mass Transfer*, **22**, No. 2, 989–1002 (1979).
12. N. N. Kochurova, "Kinetics of condensation–evaporation," in: *Heat and Mass Exchange*, Minsk Int. Forum-92, Lykov Inst. of Heat and Mass Exchange, Belorussian Acad. of Sci. (1992), Vol. 4, Part 2, pp. 101–104.
13. B. Platzer, A. Plot, and G. Maurer, *Thermophysical Properties of Refrigerants*, Springer-Verlag, Berlin (1990).
14. L. D. Landau and E. M. Lifshits, *Mechanics of Continua* [in Russian], Gostekhteoretizdat, Moscow (1954).
15. Yu. V. Afanas'ev and O. N. Krokhin, "Gas-dynamic theory of the action of laser radiation on condensed substances," *Tr. FIAN*, **52**, 118–170 (1970).
16. V. V. Korneev, "On the possibility of determining the coefficient of water condensation from evaporation experiments with a laser," *Teplofiz. Vys. Temp.*, **28**, No. 3, 536–539 (1990).
17. C. Cercignani, "Strong evaporation of polyatomic gas," in: *Rarefied Gas Dynamics*, S. S. Fisher (ed.), AIAA Paper, Part 1, New York (1981), pp. 305–320.